IEEE Trans Biometrics, Behavior and Identity Science, 2019

Towards Pose Invariant and Completely Contactless Finger Knuckle Recognition

Ajay Kumar

Abstract: *In order to advance application of finger knuckle modality in new domains, especially using widely popular smartphones, completely contactless and pose invariant knuckle identification is highly desirable. Earlier work in the literature incorporates finger knuckle images under fixed poses, which is not realistic for completely contactless biometrics applications. This paper makes first such attempt to investigate the possibility of recognizing completely contactless finger knuckle images acquired under varying poses. New approach to automatically normalize and align contactless finger knuckle images is introduced and the performance of a specialized matcher is investigated to achieve superior performance. A new database from 221 different subjects' contactless finger knuckle images is also developed and made available in public domain to advance much needed research in this area. Experimental results illustrated in this paper are promising and validate the usefulness of normalization and matching algorithms to recognize finger knuckle with different poses. Spatial and spectral domain features can provide complimentary cues and are simultaneously employed for the performance improvement. Such performance improvement serves as the baseline for much needed further improvement in recognition accuracy for database presented in this paper.*

1. Introduction

Choice of a biometrics trait highly depends on the nature of application, biometric availability and the user convenience. Finger knuckle is an emerging biometric that meets many such requirements in a variety of applications; *e.g.* for the law-enforcement when a knuckle image is the only available piece of evidence to identify suspects, privacy savvy or elderly users. Many publications in the literature have detailed experimental results that indicate high matching accuracy, or at least comparable with those from fingerprints, while using the knuckle images that are acquired under touchless imaging environment. Finger knuckle essentially represents physiological biometric pattern whose uniqueness is related to the anatomy of proximal phalanx bones, metacarpal phalanx bones, metacarpophalangeal joint and the tissues surrounding these joints. The formation of knuckle patterns can be linked to the genetics factors during the gestation stage. Several references

in the literature have identified NOG gene [1]-[2] that encodes bone morphogenetic protein which blocks further bone formation in the region of future finger joints that leads to the formation of joint space. The finger knuckle creases are developed in relation to this joint as a result of functional adaptation that requires additional skin to support the forward movement of fingers. The formation of finger joints from NOG gene indicates its relationship with the finger knuckle creases observed in our hands. The uniqueness and the formation of finger knuckle patterns is therefore largely influenced by the factors relating to functional requirements and the genetics. It is worth to mention that some diseases[*] and trauma can significantly alter appearance of knuckle patterns but this is also an issue with more established biometric modalities like fingerprint or iris.

1.1 Related Work

Finger knuckle biometrics has received increasing attention in the biometrics literature and a range of matching algorithms have been investigated to improve the matching accuracy. Earlier work [5] on knuckle biometrics incorporated finger pegs to restrict the movement of fingers and demonstrated viability of knuckle patterns for biometric modality. Contactless imaging to acquire finger knuckle patterns was later introduced [16], [20] and was another advancement towards the deployment of knuckle biometrics for online applications. Several spatial-domain and spectral-domain features have been investigated in the literature to improve matching accuracy of automatically segmented knuckle region of interest images and demonstrated with great success. There have also been attempts to classify finger knuckle patterns into several categories and these studies have been motivated by the increasing evidences for the forensic investigations from photographs involving knuckle images of suspects. In this context, the courtroom arguments also require to establish longitudinal stability of knuckle patterns. Therefore more recent study [3] that acquired knuckle images from several subjects,, among different age groups over several years

[*] Subjects with Symphalangism [11] disorder can suffer from lack of finger knuckle patterns in proximal interphalangeal joints.

were used to establish stability of knuckle patterns, particularly among the adults. Many other advancements in the finger knuckle biometrics have incorporated simultaneous acquisition of finger knuckle with finger vein [18], finger knuckle with palm dorsal surface, or finger knuckle with finger geometry that have illustrated that knuckle patterns can be utilized to further improve the accuracy for more established biometrics modalities.

There are several finger knuckle databases available in the research and reference [5] provides excellent summary of these databases. However, all these databases were acquired with requirements that one side of the finger touches with some hard surface which can ensure that the acquired images have nil or negligible scale changes. Therefore, none of these databases illustrate finger knuckle images acquired under *completely* contactless imaging. Similarly, all prior finger knuckle databases, summarized in [5], were acquired under fixed finger poses, *i.e*., user is requested to keep his/her finger straight or aligned to the imaging block. Such *fixed finger pose* requirement restricts the deformations in the finger knuckle creases (Figure 1) and fails to capture knuckle crease deformations generated under more realistic or completely contactless imaging requirements. Acquisition of completely contactless and varying pose finger knuckle also raised severe challenges, for the region of interest segmentation and matching, and this paper attempts on such advanced and also introduces a new or challenging finger knuckle database.

1.2 Motivation and this Work

Earlier work on the finger knuckle biometrics [5] have attempted to match knuckle images that are acquired under fixed poses. Many of such fixed pose finger knuckle images have delivered remarkable accuracies and beyond that is expected from many established biometrics modalities. In order to advance applicability of this biometrics modality in new domains, completely contactless and on-the-move knuckle identification is desirable. Such efforts can also help towards completely contactless finger knuckle identification using smartphones which are popularly used today. However completely contactless finger knuckle imaging often introduces pose changes

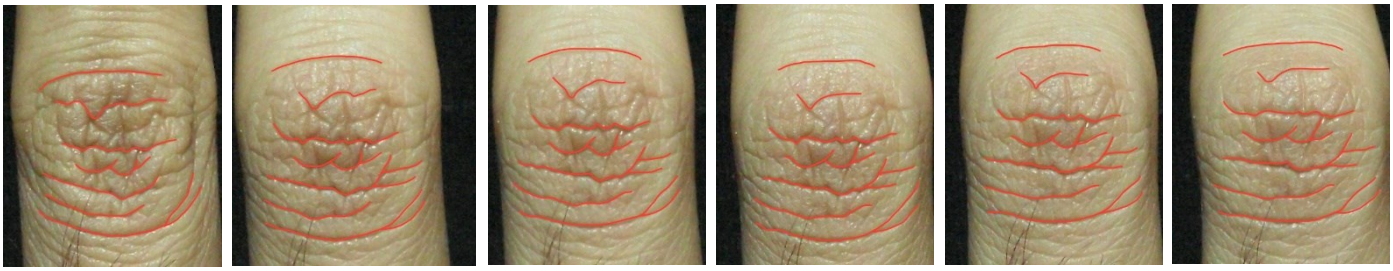

Figure 1: Finger knuckle image samples from same finger with deformations caused by varying poses. Knuckle curves in red colour are *manually* marked to illustrate variations in corresponding knuckle creases when the angle between *phalenges* is varied from zero degrees towards extreme (left to right).

which is responsible for the deformations of the knuckle patterns with pose changes. Such deformations can be observed from the images shown in figure 1. Therefore pose invariant knuckle identification is highly desirable and has not yet received attention from the researchers in the literature. There are a range of forensic images where finger knuckle region regularly feature and is often the piece of only evidence available to identify the suspects [13]-[14]. Establishing scientific evidence from such forensic images also requires capabilities to match knuckle images from different poses and is another motivation for this line of research.

This paper introduces a completely contactless finger knuckle images database from 221 different subjects where each of the knuckle images are acquired under different poses. Each of the six images from every subject, in every session, represents different finger poses that illustrate deformations in the knuckle crease patterns. A specialized and completely automated approach to segment and normalize finger knuckle images under severe deformations is developed. Finger knuckle curves are centered around the metacarpophalangeal joint and therefore local orientations from knuckle creases is incorporated to estimate such knuckle center locations under varying poses. This paper also presents a new approach to match such finger knuckle patterns using contrast context ternary feature. The experimental results presented in section 5 of this paper illustrate significant improvement in performance over competing methods presented in the literature. This performance can be further improved by incorporating spectral features and these results are also presented in the paper that serves as the baseline recognition performance for this database. Availability of this new database in public domain, along with baseline results from this

paper, will help to advance much needed research on matching completely contactless finger knuckle images under different poses.

2. Pose Invariant Finger Knuckle Imaging and Segmentation

Each of the volunteers provided finger dorsal image samples, under six different poses, from right hand index fingers. The sequence of pose variations was consistent and shown in figure 2. All the image samples were acquired using smartphones under indoor and outdoor environments. A total of 221 different subjects provided their image samples in the first session. For the second session imaging, only 104 subjects were available. One of the key challenges in the development of completely automated pose invariant finger knuckle identification is to segment region of interest images that can adequately/only represent knuckle crease patterns. This region of interest is the

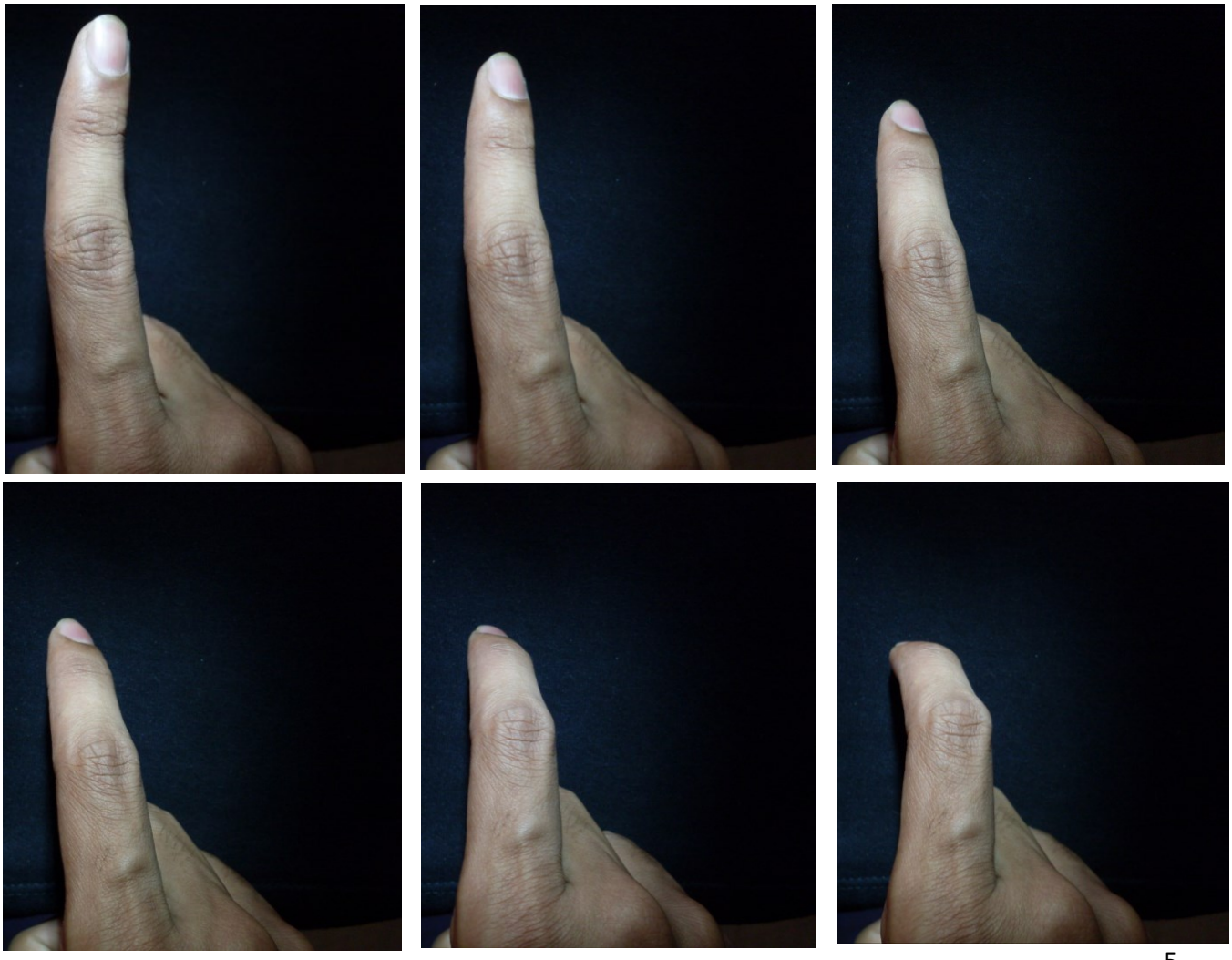

Figure 2: Finger dorsal image samples were acquired using a smartphone from the index finger of 221 different subjects and each of the different subject provided image samples with six different poses under completely contactless imaging under ambient illumination.

sub image region that represents finger dorsal skin crease patterns between the medial and the proximal phalanx finger joints.

Each of the acquired images are firstly cropped to generate a fixed ROI images from the spatial image center and resulting images are subjected to the segmentation steps as shown in figure 3. An edge detector is employed to extract finger shape boundaries. The slope of resulting finger shape curve is used to estimate the finger orientation for the alignment. Completely contactless imaging results in images that can have high intra-class scale variations and therefore scale normalization is essential part of pre-processing operations. Another important purpose for estimating the scale of the image is for the selection of appropriate parameters, *e.g.* for the image enhancement and the knuckle crease center estimation process. The scale of the imaged fingers for the normalization is estimated by computing the width of the fingers. In order to ensure that the (smaller) fingers does not include nail regions in the estimation of such scale, small region from the top/tip is ignored during the estimation of finger width for the normalization. The scale normalization step ensures that the segmented region of interest images have same width. Contactless knuckle images under ambient illumination illustrate degrades the image contrast and therefore the resulting images are subjected to enhancement. This final step or the image enhancement operation is same as employed in several references, *e.g.* [3]. Average of illumination in 30 × 30 different blocks is used to estimate the illumination profile which is subtracted from original knuckle image and the resulting image is subjected to histogram equalization.

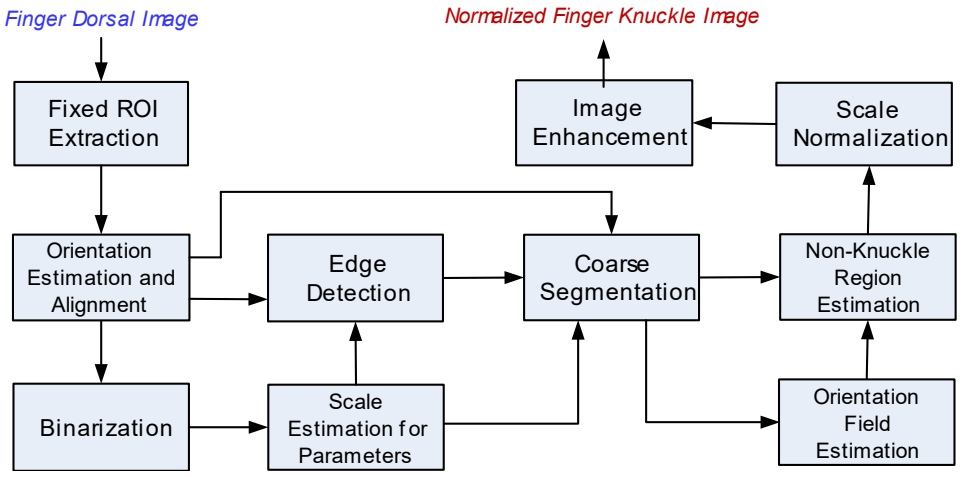

Figure 4: Block diagram representing different steps in the automated segmentation of region of interest images from the acquired finger knuckle images.

3. Detecting Knuckle Crease Flow Center

Finger knuckle flow patterns generally illustrate multiple and wide ridges, with varying thickness, that are separated by narrow valleys. These ridge flow patterns are centered at metacarpophalangeal joint, *i.e.*, joint between proximal and metacarpal phalanx bones. Automated estimation of such *knuckle center* can help to align region of interest during the feature extraction and matching process. Therefore, the estimation of such knuckle image center is developed and detailed in this section.

The orientation flow map of the curved knuckle lines and creases is firstly estimated from the normalized knuckle images. There are several methods in the literature [12], [15] to compute the orientation field of textures. Each of the knuckle images are divided into blocks of size $w \times w$ pixels. The local orientation map of knuckle curves at point (x, y) can be computed as follows:

$$\mathrm{J}_x(x,y) = \sum_{p=x-\frac{w}{2}}^{x+\frac{w}{2}} \sum_{q=y-\frac{w}{2}}^{y+\frac{w}{2}} 2\mathrm{G}_x(p,q)\mathrm{G}_y(p,q) \tag{1}$$

$$\mathrm{J}_y(x,y) = \sum_{p=x-\frac{w}{2}}^{x+\frac{w}{2}} \sum_{q=y-\frac{w}{2}}^{y+\frac{w}{2}} \left(\mathrm{G}_x^2(p,q) - \mathrm{G}_y^2(p,q)\right) \tag{2}$$

$$\theta\,(x,y) = \frac{1}{2} tan^{-1}\left(\frac{\mathrm{J}_x(x,y)}{\mathrm{J}_y(x,y)}\right) \tag{3}$$

where $\mathrm{G}_x(x,y)$, $\mathrm{G}_y(x,y)$ represents the gradients for pixels positioned at (x, y) and the estimated angle of orientation is $(\theta\,(x,y) + \pi/2)$ since gradient vector $\overrightarrow{\mathrm{n_i}}$ (figure 4) is perpendicular [15] to

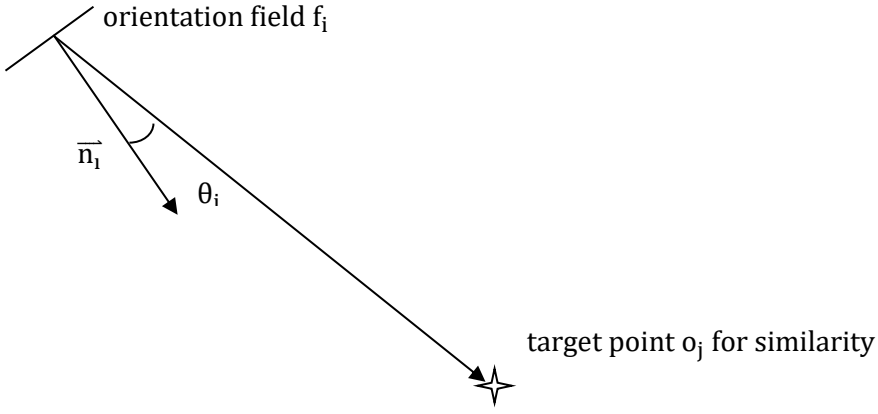

Figure 4: Illustration of the angle θ_i representing the difference between orientations of knuckle curve at point o_j and respective orientation at point f_i where $\overrightarrow{\mathrm{n_i}}$ is the estimated normal vector from the orientation field.

the direction of anisotropy. After computing the direction map with respect to the principle axis of variation from the image gradients, using the normalized and enhanced knuckle ROI image, a fitness score is computed for *each* of the point in respective image. This fitness score represents possibility that the knuckle center lies at a given point (x, y) in the normalized knuckle image.

The angle of intersection or similarity with the orientation at point $o_j(x, y)$, from the orientation field $f_i(x, y)$ at any arbitrary point in the knuckle image is computed as shown in figure 4. The fitness score s_{o_j} at every point in the image is computed from the summation of $\cos\theta_i$ contributions from all other orientation fields in the different image blocks.

$$s_{o_j} = \sum_i \cos\theta_i \tag{4}$$

In order to establish the center point of the knuckle image, the spatial locations of top five points with highest scores are considered. The knuckle center is estimated from the arithmetic mean value

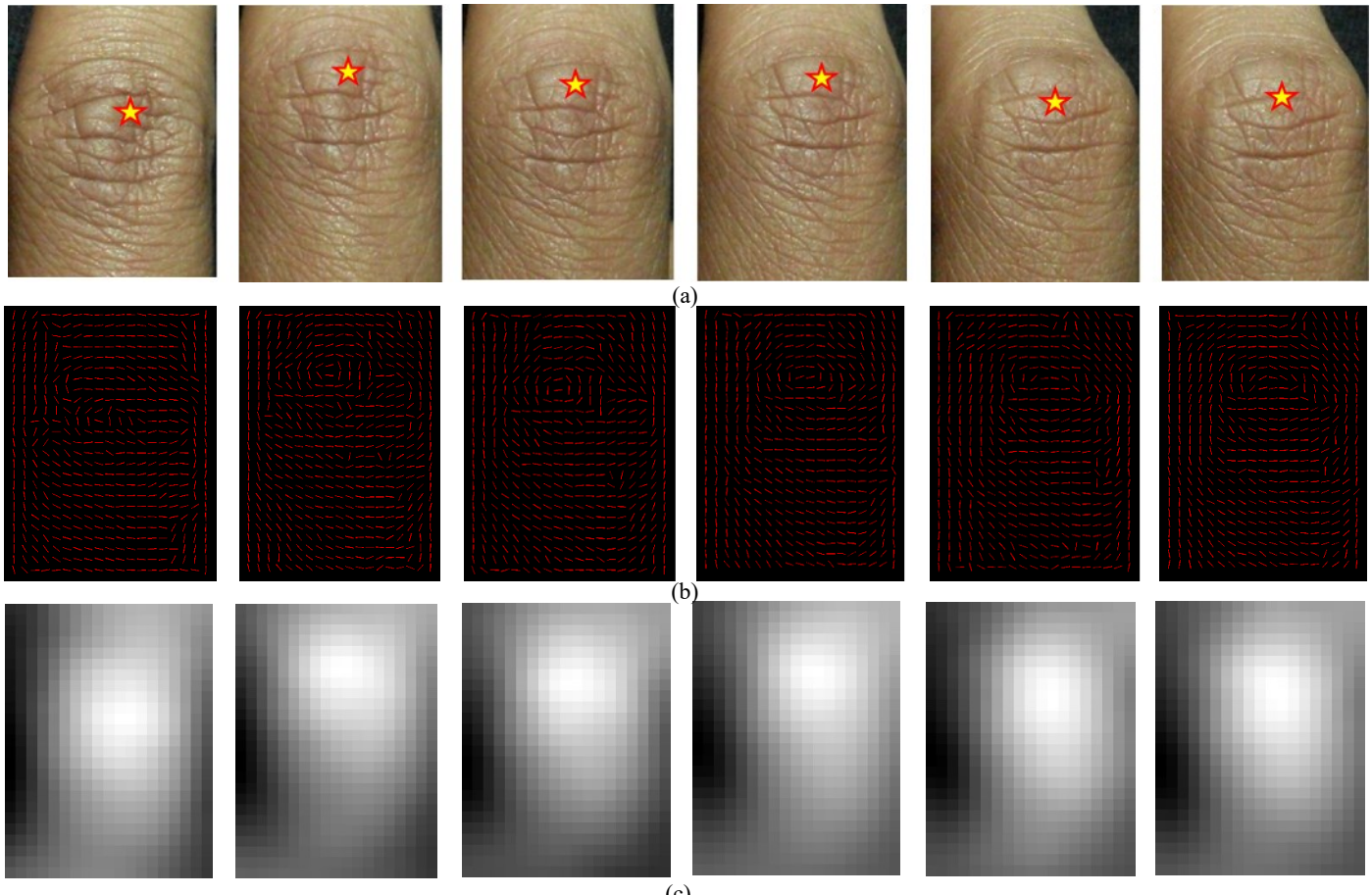

Figure 5: (a) Sample normalized finger knuckle images with respective six different poses, (b) corresponding local orientations estimated in each of 19 × 25 blocks, (c) fitness score representations in each of the corresponding blocks. The location of knuckle center, automatically computed from the fitness scores in (c), is shown as *star* and is overlaid on original normalized knuckle sample images in (a).

of the positions of these points. The knuckle center point is useful for the registration of different knuckle images. Figure 5 illustrates a finger knuckle with different poses and the estimated knuckle center along with the fitness scores. It can be observed from results in figure 5 that the estimation of knuckle center is quite stable in these images with varying poses.

4. Feature Extraction and Matching

There are ranges of spatial and spectral feature extraction methods that can be employed to match normalized finger knuckle images. However, the contactless knuckle images in this database have significant variations in the poses. Therefore, the feature extraction methods that can encode aggregate information from curved regions were focus of this investigation for superior performance. A new spatial-domain approach to match normalized finger knuckle images is developed. This approach is motivated by the effectiveness of contrast context histogram features in [9] and is detailed in the following.

The contrast context histogram (CCH), at the knuckle center computed from the method detailed in previous section, is firstly computed. Let A_c (x_c, y_c) be such knuckle center point, and A (x, y) represent one point in the local region surrounding A_c. The CCH can be estimated as follows [9]:

$$C(A) = I(x, y) - I(x_c, y_c) \tag{5}$$

where I(x, y) and I(x_c, y_c) represents respective gray level intensity values. When C(A) > 0 the estimated contrast have positive values otherwise it represents negative contrast values. The local region centered at knuckle center A_c is partitioned into 24 blocks, which represents the local regions from eight 8 different directions and three different radius. The spatial distribution of these different regions is shown in figure 6. Let us represent these different knuckle regions with R_i with i = 1 .. 24. For every point A in the region R_i, we can define the contrast histogram bin with respect to A_c as follows:

$$H_{R_i^+}(A_c) = \frac{\sum\{C(A) | A \in R_i \text{ and } C(A) > 0\}}{N_{R_i^+}} \tag{6}$$

$$D_{R_i}{}^{+}(A_c) = \frac{N_{R_i}{}^{+}}{N_{R_i}} \tag{7}$$

$$H_{R_i}{}^{-}(A_c) = \frac{|\Sigma\{C(A)|A \in R_i \text{ and } C(A) < -0\}|}{N_{R_i}{}^{-}} \tag{8}$$

$$D_{R_i}{}^{-}(A_c) = \frac{N_{R_i}{}^{-}}{N_{R_i}} \tag{9}$$

where $N_{R_i}{}^{+}$ represents the number of positive contrast values in respective region R_i , while $N_{R_i}{}^{-}$represents the number of negative contrast values in corresponding region R_i, N_{R_i}represents the number of all points in R_i while $D_{R_i}{}^{+}$indicates ratio of number of pixels whose intensity is larger than those for point A_c in given knuckle sub-region. Comparative evaluation of $H_{R_i}{}^{+}, H_{R_i}{}^{-}, D_{R_i}{}^{+}, D_{R_i}{}^{-}$with T_H, T_D respectively can used to generate the ternary code T as follows:

$$T_i = \begin{cases} 1 & H_{R_i}{}^{+} > T_H \text{ and } D_{R_i}{}^{+} > T_D \\ -1 & H_{R_i}{}^{-} > T_H \text{ and } D_{R_i}{}^{-} > T_D \\ 0 & \text{Otherwise} \end{cases} \quad \text{for } i = 1..N \tag{10}$$

In order to avoid the ambiguity that T_i can have both 1 and -1 values, T_D should be set larger or the same as 0.5. The values for T_D and T_H are empirically fixed as 0.5 and 0.1 respectively. Encoded values of T_i can be used to compute the match score between the two knuckle images. The match score between two such bits in ternary contrast context vector (TCCV) can be computed as follows:

$$D(T_1, T_2) = -|T_1 - T_2| + 1 \tag{11}$$

The outcome from above equation is systematically detailed in Table 1 below.

Table 1: Lookup table for match score between two ternary bits.

T_1	T_2	$D(T_1,T_2)$
1	1	1
1	0	0
1	-1	-1
0	0	1
0	-1	0
-1	-1	1

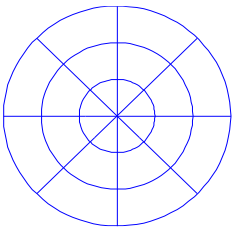

Figure 6: Localization of 24 sub-regions around the center point.

Let P and Q respectively denote the matrix of corresponding vectors from the two arbitrary knuckle images, each with the image size of M × L. The consolidated match score between these two normalized knuckle images can be computed as follows:

$$S(P,Q) = \frac{\sum_x \sum_y \sum_{k=1}^{N} (D(P_k(x,y), Q_k(x,y))}{N * L * M} \quad (12)$$

This match score lies in 0-1 range and the best-case match score is expected to be one.

5. Database and Experimental Results

Images from completely contactless and finger knuckle with six different poses were acquired from the volunteers using different smartphones. These images were acquired in indoor and outdoor environment under a relatively fixed background. All the volunteers were requested to present their index fingers under six different poses with first images representing the image when finger is straight while the last/sixth image representing the image when finger is bent excessively while ensuring that the knuckle region stays within the focus of the smartphone camera. This arrangement also helps to automatically extract region of interest representing knuckle images from the acquired images. Figure 2 illustrates sample image from a volunteer. None of the volunteers were paid or presented with any gifts for their help in providing the images for this research. The volunteers contributing the images in this database had varying skin pigmentation. This database over a period of three years. Among these 221 different subjects, 104 subjects also provided their knuckle images after an interval of eight weeks (minimum). Therefore a total of 1950 different knuckle images acquired from six different index finger poses and the entire dataset is publicly made available [7] to advance further research in this area. Figure 7 illustrates another

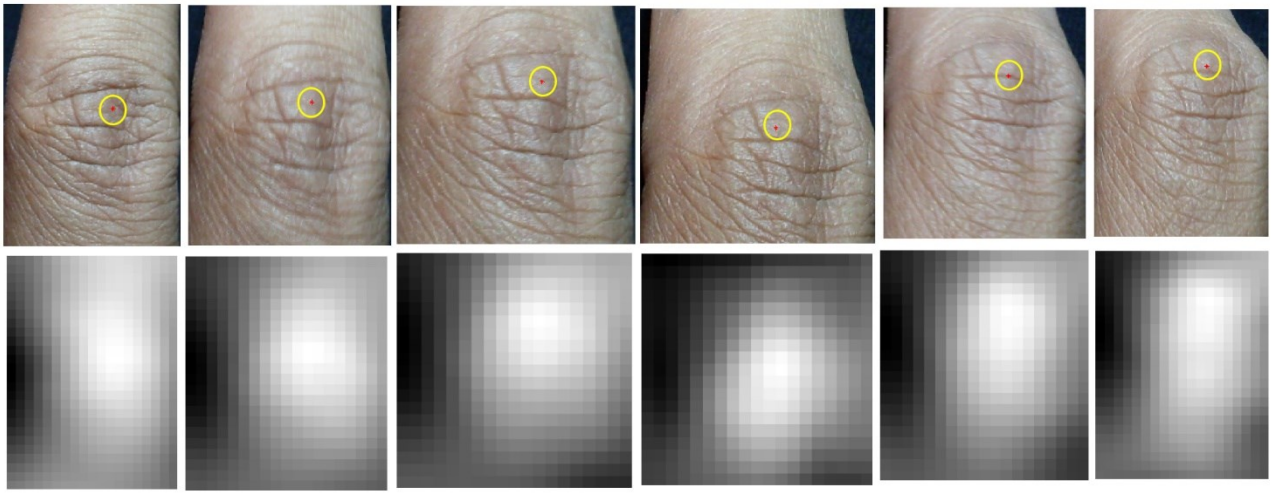

Figure 7: Sample normalized finger knuckle images with respective six different poses and corresponding fitness score representations in each of the corresponding blocks. The location of knuckle center, automatically computed from the fitness scores and marked on original normalized knuckle sample images (red dot inside yellow color circle).

sample of normalized finger knuckle image from a subject in this database, along with its automatically extracted knuckle center. The knuckle center of each of the image extracted using the method detailed in section 3, along with segmented ROI images, are publicly made available *along with* this database.

The feature extraction using TCCV (developed in section 4) a Difference of Gaussian (DoG) filtering with two Gaussian kernels whose parameters were empirically fixed (filter length =22, $\sigma_1 = 4,\ \sigma_2 = 0.7$) for all the normalized knuckle images in the database. Knuckle image enhancement step employed 30 × 30 block size for the estimation of (uneven) illumination profile. There are range of other spatial domain methods that have shown to offer competing performance on finger knuckle images and were also attempted to comparatively ascertain the performance. These methods include local binary patterns (LBP) [17], local ternary patterns (LTP) [19], multi-LBP [17], local derivative patterns (LDP) [8], binary orientation co-occurrence vector (BOCV) [6] and local feature descriptor (LFD) [3] which has shown to offer superior performance over many other feature descriptors. The parameters for these methods were empirically determined and set to achieve best performance for this database. For the LBP, 4 × 4 block size with radius of 9 was used while multi-LBP approach used radius values of 5, 7 and 9. The experiments with LDP used 3 × 3 blocks with a step size of 18. The experiments using BOCV [6] used block size of 49 × 49 with 0.06 and 0.3 thresholds to achieve best possible performance. Figure 8 illustrates a sample normalized finger knuckle image along with its gray-level representation of different feature extraction methods considered in this work.

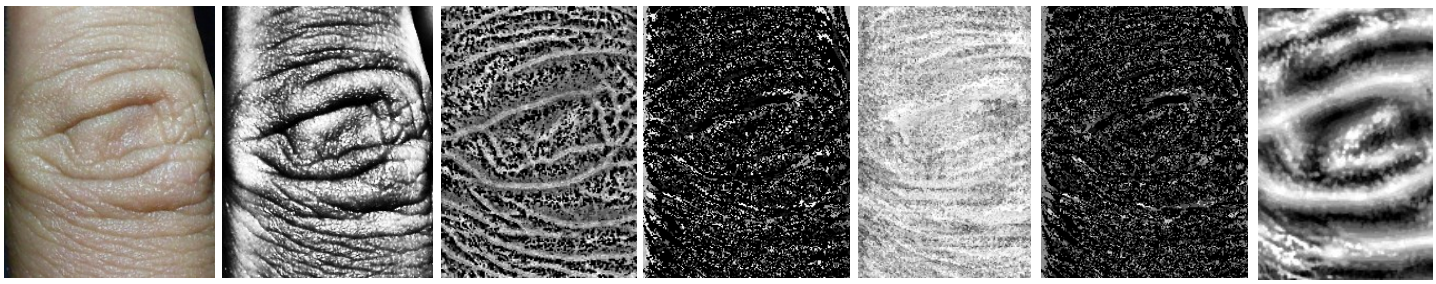

(a) (b) (c) (d) (e) (f) (g)

Figure 8: Two sample normalized knuckle images in the new database (a), respective enhanced images (b), gray-level feature map representations using BOCV (c), LBP (d), LDP (e), LTP (f) and (g) TCCV in this paper.

In the first set of experiments, the second session database was used to compute average recognition accuracy for all 104 subjects in this part of database. Table 2 summarizes average rank-one recognition accuracy (0-1 range) from different methods. It can be observed that TCCV achieves superior performance than other baseline methods considered in this work. The first session database was acquired from 221 different subjects and therefore average recognition accuracy, using leave-one-out approach, from different methods was also computed and is summarized in Table 3. These results also underline the effectiveness of TCCV approach introduced in section 4.

Table 2: Comparative performance for two session database using spatial domain features.

Matcher	[6]	LDP	LTP	Multi-LBP	[3]	TCCV
Average *Rank-one* rate	0.4840	0.2885	0.4744	0.5160	0.4038	**0.5337**

Table 3: Comparative performance from first session database using spatial domain features.

Matcher	[6]	LDP	LTP	Multi-LBP	LFD [3]	TCCV
Average Rank-one rate	0.8137	0.6900	0.8077	0.8575	0.6261	**0.8680**

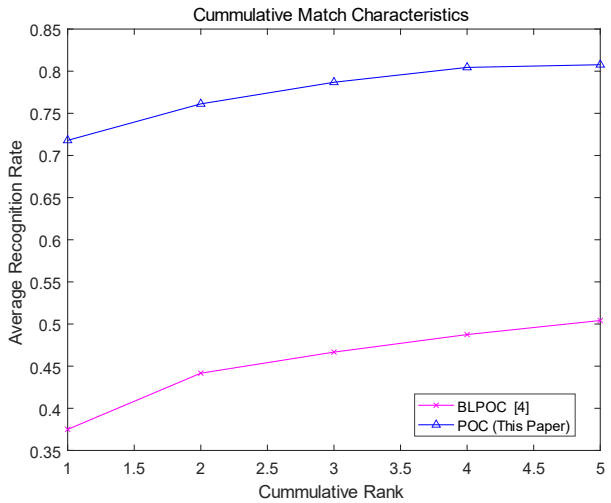

Figure 9: Comparative recognition performance from spectral features using two-session normalized knuckle images.

Fourier representation of images is known to be least sensitive to translational and rotational changes in the images. Therefore spectral domain feature representation was also attempted to

compute the similarity of normalized knuckle images using phase correlation function [10]. Band limited phase only correlation [4] recovers phase information from the 2D discrete Fourier transform (DFT) and has shown to offer promising results for finger-knuckle matching. Therefore, this approach was also comparatively evaluated for the recognition performance using two-session normalized finger knuckle images. As can be observed from results in this figure, phase only correlation (POC) provides superior performance using spectral domain feature representation and was the preferred choice to investigate further performance improvement. Spectral and spatial features can provide complimentary information and simultaneously extracted from the normalized knuckle images. The best performing spatial-feature match scores from TCCV and spectral-feature match scores from POC were simultaneously combined to achieve best possible performance from this database. Figure 10 illustrates recognition performance from best performing spatial and spectral domain approach using cumulative match characteristics (CMC) The performance from two-session protocols are illustrated in figure 10(a) while those from first session database are illustrated in figure 10(b). These results indicate that the simultaneous usage and recovery of spectral and spatial features can offer significant improvement in the performance.

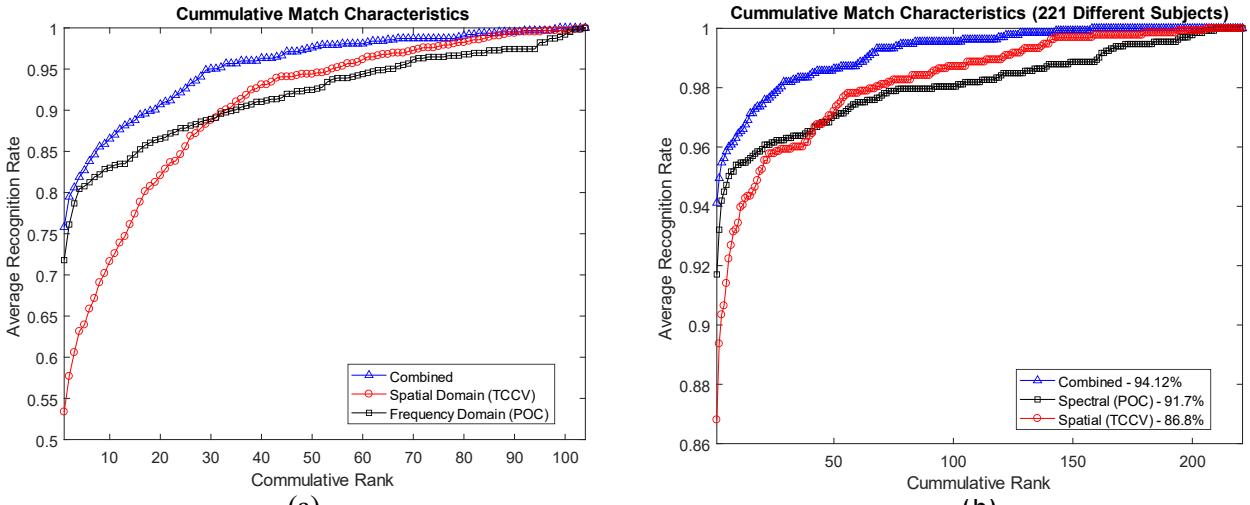

Figure 10: Comparative recognition performance using simultaneously extracted spatial and spectral domain features, (a) using two-session database from 104 subjects and (b) one-session database from 221 subjects.

6. Discussion

The LBP and LFD are known to be invariant to monotonic gray-level transformations. However, such approaches are expected to be sensitive to the noise in the image regions with nearly uniform gray levels. This can be attributed to the thresholding operation in LBP (thresholding by comparison with the gray level at local block center) and also in BOCV and LFD. In order to overcome such limitations, ternary feature representation was investigated. Such three-value codes generated from TCCV in (10) in this paper are expected to be more resistant to the noise and weak illumination gradients, which is especially important for completely contactless knuckle images acquired under ambient illuminations as in this database. Experimental results presented in Table 1-2 can validate the effectiveness of such approach over other competing methods considered in this work. It should be noted that TCCV uses knuckle crease center estimation (section 3) from deformed creases, which is not required or employed for knuckle images available in other fixed finger pose finger knuckle databases. More importantly, TCCV encodes *aggregate* contrast from the deformed knuckle patterns image sub-regions while knuckle images in fixed pose databases can directly benefit from the direct comparisons between the pixel-wise features (*e.g.* as for methods in [3]). Therefore TCCV is not expected to outperform on fixed pose finger knuckle databases [5], as earlier matching methods benefit from the absence of severe finger knuckle crease deformations.

The spectral domain approaches like POC or BLPOC require 2D-DFT operations which are known to be computationally complex. Therefore, spatial approach using TCCV can offer be much faster alternative and attractive choice for the online applications. The height of phase correlation is employed in POC, using inverse of 2D-DFT, to ascertain the similarity between two matched knuckle images [10]. The BLPOC [4] eliminates high frequency components in the computations of such cross-phase spectrum. These high-frequency components can however provide some cues to establish similarity between matched knuckle images from different poses in our experiments. This can be a plausible reason for the superior performance from POC, over BLPOC, from the experimental results in section 6.

The knuckle center estimation introduced in section 3 helps to alight different ROI knuckle images. Sample results in figure 6-7, indicate that this approach is quite effective, especially considering for the nature of contactless knuckle images under ambient illumination. The accuracy of this approach however depends on the accuracy of region of interest detection which itself is challenging under completely contactless image acquisition using mobile phones. It is useful to note that the accuracy in the computation of knuckle crease center also depends on the chose size of image blocks. Figure 11 illustrates poor examples of automatically detected and segmented finger knuckle images using the method introduced in section 2. However, the failure of knuckle region in these samples cannot be just attributed to the limitations of the knuckle segmentation method as many of these images presented by volunteers were inconsistent and not in line with the guidelines. Completely contactless imaging provides enormous freedom and lack of any incentive for the volunteers contributing image samples have enriched this database with several challenges that needs to be addresses in the further extension of this work.

Figure 11: Sample region of interest images depicting limitations of the approach investigated in this work.

7. Conclusions and Further Work

This paper introduces first *completely* contactless finger knuckle database, which provides knuckle images from varying poses that are acquired in two-sessions. This database has been acquired from 221 different subjects and motivated by the pressing need to develop pose invariant finger knuckle recognition capabilities for the civilian, forensic and surveillance applications. Entire database, along with segmented region of interest images, is publicly made available [7] to advance this line of research. This paper also introduced a new approach to match pose varying finger knuckle images and the experimental results presented in section 5 validate the effectiveness of this

approach. Combination of spatial and spectral domain approach presented in this paper have helped to further improve the performance and serve as the baseline recognition performance from this database.

The average recognition accuracy from the two-session database achieved (75.83%) in this work is poor and needs further work for the deployment of pose invariant knuckle recognition in forensic and civilian applications. The images shown in figure 11 also indicate that the automated segmentation/detection of finger knuckle region of interest, under completely contactless and varying poses, is a challenge and more effective methods needs to be developed to achieve performance improvements. Such detection can be more accurately performed by using a trained detector, such as the contactless palmprint detector in [22] or the iris detector in [23]. Such trained detector using convolutional neural network can be especially be helpful under the complex imaging backgrounds, as widely observed under real forensic or surveillance images, and is suggested for further work. The test protocols used for the experiments in this paper, either for the single session (leave-one-out) or two-session experiments, use all or six different poses for the registration or training and therefore not challenging to meet expectations for the real deployments. Only one image with any of the six different poses (figure 1) should be utilized for the training and average recognition accuracy should be reported on the rest of the images, either from the same or different session images, to ascertain algorithmic performance. Such protocols are detailed along with this public database [7] and should be employed to advance pose-invariant finger knuckle capabilities for the real deployments.

The database introduced in this paper illustrate images with varying information in finger dorsal regions. As can be observed from the sample images in figure 2, some finger dorsal images present minor finger knuckle regions and nails while these details are occluded in images with significant pose changes. Some of these *additional* finger dorsal region details can be utilized to improve the recognition performance and suggested for further work. The work in this paper has been limited to ascertain *recognition* performance which may not indicate [21] expected

performance for the verification problem. Therefore, further extension of this work should also investigate verification performance from the challenging database presented in this paper.

Acknowledgements

Author thankfully acknowledges great support from all the volunteers and research assistants who have helped in the development of completely contactless finger knuckle database detailed in this paper.

References

[1] Y. Gong, D. Krakow, J. Marcelino, D. Wilkin, D. Chitayat, R. Babul-Hirji, L. Hudgins, C. W. Cremers, F. P. Cremers, H. G. Brunner, K. Reinkers, D. L. Rimoin, D. H. Cohn, F. Goodman, W. Reardon, M. Patton, C. A. Francomano, and M. L. Marman, "Heterozygous mutations in the gene coding noggin affect human joint morphogenesis," *Nature Genetics,* vol. 21**,** pp. 302-304, 1999.

[2] L. B. Zimmerman, J. M. De Jesus-Escobar, and R, M. Harland, "The Spemann organiser signal Noggin binds and inactivates bone morphogenic protein 4," *Cell,* vol. 86, pp. 599-606, 1996.

[3] A. Kumar and Z. Xu, "Personal identification using minor knuckle patterns from palm dorsal surface," *IEEE Trans. Info. Forensics & Security*, pp. 2338-2348, Oct. 2016.

[4] K. Ito, T. Aoki, H. Nakajima, K. Kobayashi, T. Higuchi, "A palmprint recognition algorithm using phase-only correlation," *IEICE Trans. Fundamentals of Electronics, Communications and Computer Sciences*, vol. E91-A, pp. 1023-1030, April 2008.

[5] G. Jaswal, A. Kaul, and R. Nath, "Knuckle print biometrics and fusion schemes – overview, challenges, and solutions," *ACM Transactions. ACM Computing Surveys*, vol. 49, no. 2, Article 34, Nov. 2016.

[6] Z. Guo, D. Zhang, L. Zhang, W. Guo, "Palmprint verification using binary orientation co-occurrence vector," *Pattern Recogn. Lett*., vol. 30, pp. 1219–1227, 2009.

[7] The Hong Kong Polytechnic University Contactless Finger Knuckle Images Database (Version 3.0), https://www4.comp.polyu.edu.hk/~csajaykr/fn2.htm, 2019.

[8] B. Zhang, Y. Gao, S. Zhao J. Liu, "Local derivative pattern versus local binary pattern: Face recognition with high-order local pattern descriptor," *IEEE Trans. Image Process*. 19, pp. 533–544, 2010.

[9] C.-R. Huang, C.-S. Chen and P.-C. Chung, "Contrast context histogram – an efficient discriminating local descriptor for object recognition and image matching," *Pattern Recognition*, vol. 41, pp. 3071-3077, 2008.

[10] C. D. Kuglin and D. C. Hines, "The phase correlation image alignment method," *Proc. Intl. Conf. Cybernetics and Security*, pp. 163-165, 1975.

[11] K. Lehmann, P. Seemann, J. Boergermann, G. Morin, S. Reif, P. Knaus, and S. Mundlos, "A novel R486Q mutation in BMPR1B resulting in either a brachydactyly type C/symphalangism-like phenotype or brachydactyly type A2," *European J. Human Genetics*, vol. 14, pp. 1248-1254, 2006.

[12] M. Kass and A. Witkin, "Analyzing oriented patterns." *Proc. Computer Vision, Graphics and Image Processing*, vol. 37, pp. 362-385, 1987.

[13] A. R. Rao and R. Jain, "Analyzing oriented textures through phase portraits," *Proc. ICPR*, pp. 336-340, 1990.

[14] F. M. Vilnrotter, R. Nivatia, and K. E. Price, "Structural analysis of natural textures," *IEEE Trans. Pattern Anal. Mach. Intell.*, vol. 8, pp. 76-89, Jan. 1986.

[15] A. R. Rao, *A Taxonomy for Texture Description and Identification*, Springer-Verlag, New York, 1990.

[16] D. L. Woodard and P. J. Flynn, "Finger surface as a biometric identifier", *Computer Vision and Image Understanding*, vol. 100, no. 3, pp. 357-384, Dec. 2005.

[17] T. Ojala, M. Pietikäinen, and T. Mäenpää, "Multiresolution gray-scale and rotation invariant texture classification with local binary patterns," *IEEE Trans. Pattern Anal. Mach. Intell.*, vol. 24, no. 7, pp. 971-987, 2002.
[18] W. Yang, G. Ma, F. Zhou, Q. Liao, "Feature-Level fusion of finger veins and finger dorsal texture for personal authentication based on orientation selection," *IEICE Trans. Info. & Sys*., 97-D(5), pp. 1371-1373, 2014.
[19] X. Tan and B. Triggs, "Enhanced local texture feature sets for face recognition under difficult lighting conditions," *IEEE Trans. Image Process*., vol. 19, pp. 1635-1650, Jun. 2010.
[20] A. Kumar and Ch. Ravikanth, "Personal authentication using finger knuckle surface," *IEEE Trans. Info. Forensics & Security*, vol. 4, no. 1, pp. 98-110, Mar. 2009.
[21] R. Bolle, J. Conell, S. Pankanti, N. Ratha, "The relationship between the ROC-Curve and the CMC," *Proc. AutoID 2005*, pp. 15-20, 2005.
[22] Y. Liu and A. Kumar, "A deep learning based framework to detect and recognize humans using contactless palmprints in the wild," https://arxiv.org/pdf/1812.11319, Dec 2018
[23] Z. Zhao and A. Kumar, "A deep learning based unified framework to detect, segment and recognize irises using spatially corresponding features," *Pattern Recognition*, vol. 93, pp. 546-557, Sep. 2019.